# Using Theory to Reinterpret the Kinetics of Monofunctional Platinum Anticancer Drugs: Stacking Matters

Daniele Veclani,[†] Andrea Melchior,[*†] Marilena Tolazzi,[†] and José P. Cerón-Carrasco[*‡]

[†]Dipartimento Politecnico di Ingegneria e Architettura (DPIA), Laboratori di Chimica, Università di Udine, via delle Scienze 99 33100 Udine [‡]Bioinformatics and High-Performance Computing Research Group (BIO-HPC), Universidad Católica San Antonio de Murcia (UCAM), Campus de los Jerónimos, 30107, Murcia, Spain.

## 1. Computational details

On the basis of a large number of experimental data,[1] it is widely accepted that the reactions of Pt(II) anticancer drugs (i.e. cisplatin, **cisPt**) are initiated by a square-planar complex. That reactant is subsequently converted to a bipyramidal (5-coordinated) transition state, in which the incoming water molecule and the leaving ligands are weakly bound to the metal. The structural features of this trigonal bipyramid are relevant for determining the hydrolysis activation barrier. Calculations were carried out for the separated reactants (R), the reactant adducts (RA, the adduct between the platinum complex and the incoming nucleophile), transition states (TS), product adducts (PA, the substituted complex and the leaving group) and the products (P). All DFT calculations were performed using the B3LYP functional, composed of Becke's three-parameter hybrid exchange functional (B3)[2] and the correlation functional of Lee, Yang, and Parr (LYP),[3] using Gaussian 16 program.[4] Previous works have shown that B3LYP hybrid density functional provides reliable results for thermochemistry and kinetics of organometallic compounds.[5–16] The reactivity was also investigated including the Grimme's[17] dispersion contribution correction (B3LYP-D3) and the range-separated dispersion corrected ωB97X-D functional[18]. Geometry optimizations were carried out in vacuum with a 6-311+G(d,p) basis set for all atoms except the platinum atom, which was described by the quasi-relativistic Stuttgart-Dresden pseudopotential (SDD).[19] Since

No imaginary frequencies were obtained for the products and reactants, while a single imaginary frequency was obtained for the TS. Free energies have been calculated by adding the zero-point energy and thermal correction terms to the electronic energy of the complex. Due to the key role of solvation in influencing thermodynamic and kinetic parameters in platinum complex reactivity,[1,20–22] environmental effects have been introduced by the polarizable continuum method (PCM).[23] In this case, the energies have been recalculated in PCM water at the coordinates corresponding to the stationary points obtained in gas phase. The constrained ONIOM[24] optimization in gas phase (QM/QM') has been used to study the interaction between phenanthriplatin (**phenPt**) and DNA fragment (GGG) characterized by three base pairs. The starting structure of the three base pairs fragment has been obtained from the X-Ray diffraction data 4Q8F reported in protein data bank database. The system was divided in two layers: one containing the **phenPt** and one molecule of guanine (fully relaxed B3LYP layer) and the other corresponding to the rest of the DNA kept frozen in space and treated with the semiempirical (QM') PM6 method.[25]

## 2. Optimized chemical structures

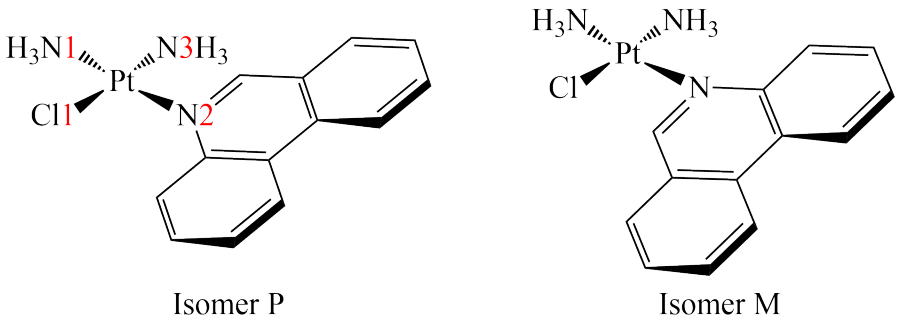


Isomer P Isomer M

**Figure S1** Structures of the two possible **phenPt** isomers, labeled as P and M depending on the orientation of the phenanthridine ring.

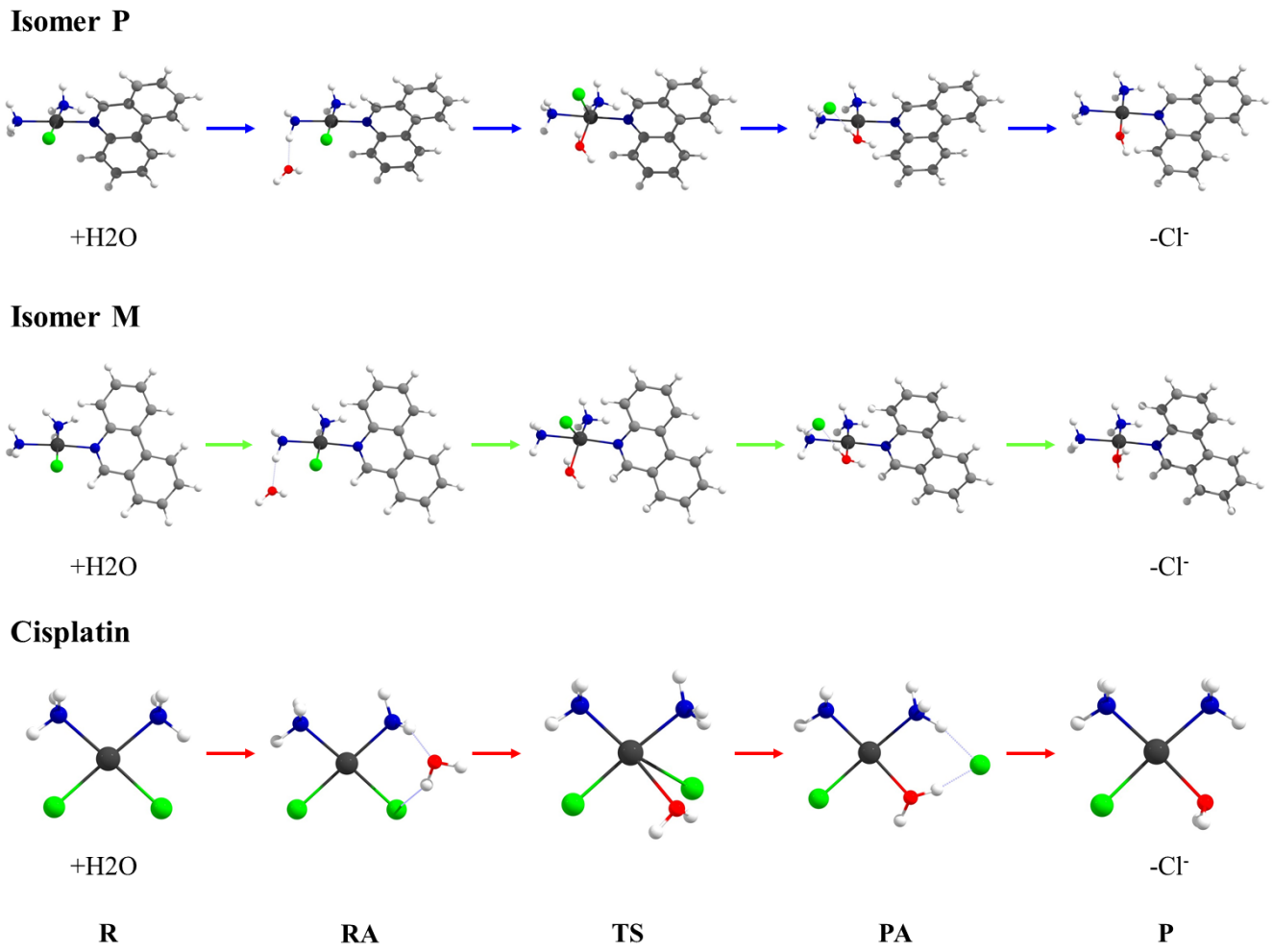


**Figure S2**. Optimized Structures of the species involved in the hydrolysis reactions of **phenPt** and **cisPt**.

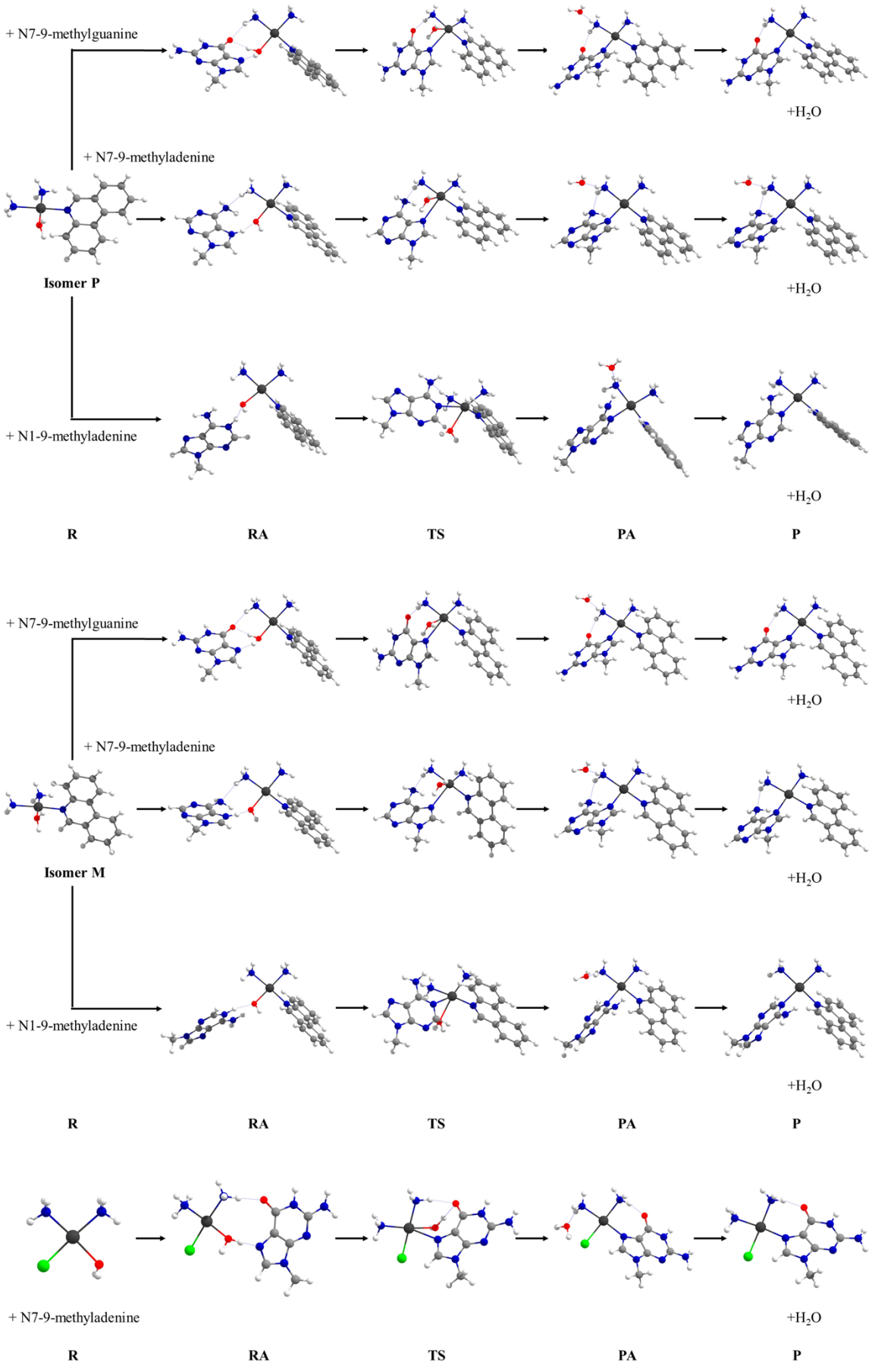


**Figure S3** Optimized structures for the reaction between bases and isomer **phenPt**-P, isomer **phenPt**-M and **cisPt**.

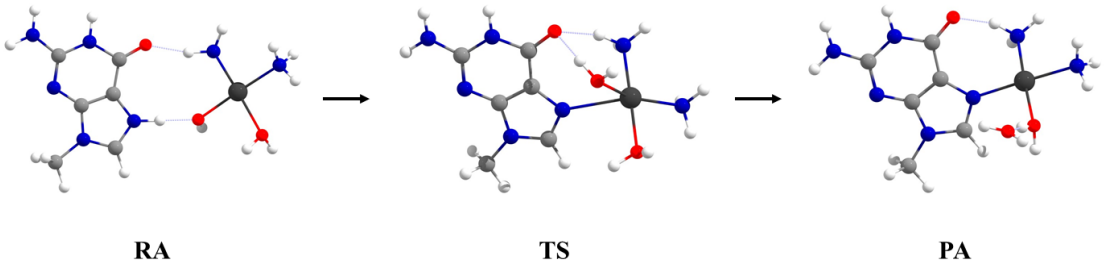


**Figure S4** Optimized structures for the reaction between N7-Me-gua and di-*acquo* complex of **cisPt**.

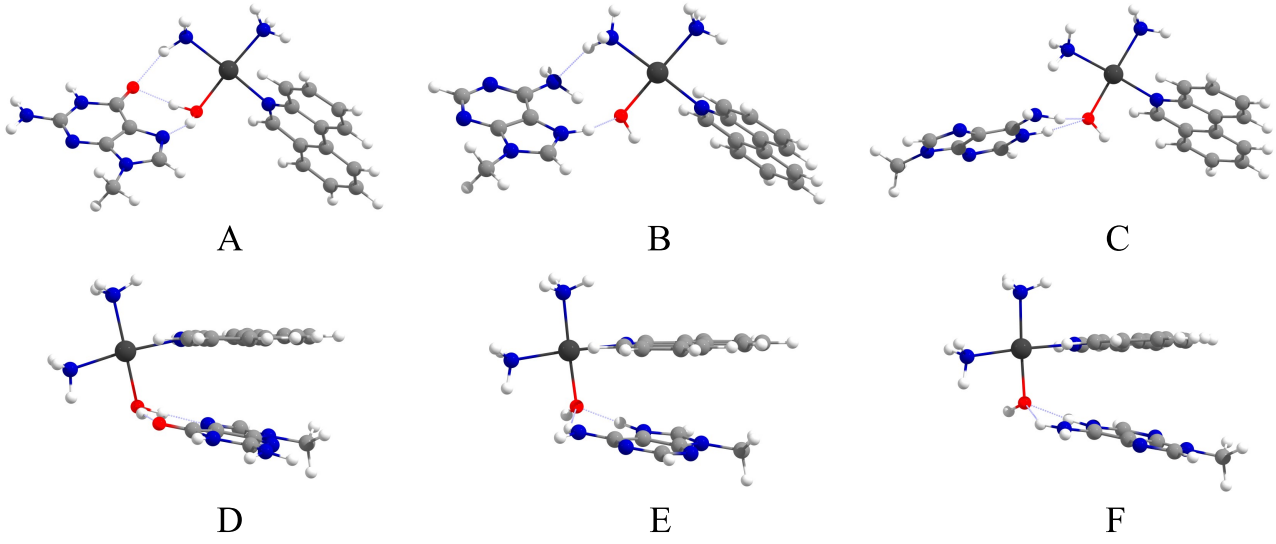


**Figure S5** Optimized structures for the RA of isomer M when the bases do not interact via π-π: A reaction with N7-Me-Gua; B reaction with N7-Me-Ade; C reaction with N1-Me-Ade, and when the bases do not interact via π-π: D reaction with N7-Me-Gua; E reaction with N7-Me-Ade; F reaction with N1-Me-Ade.

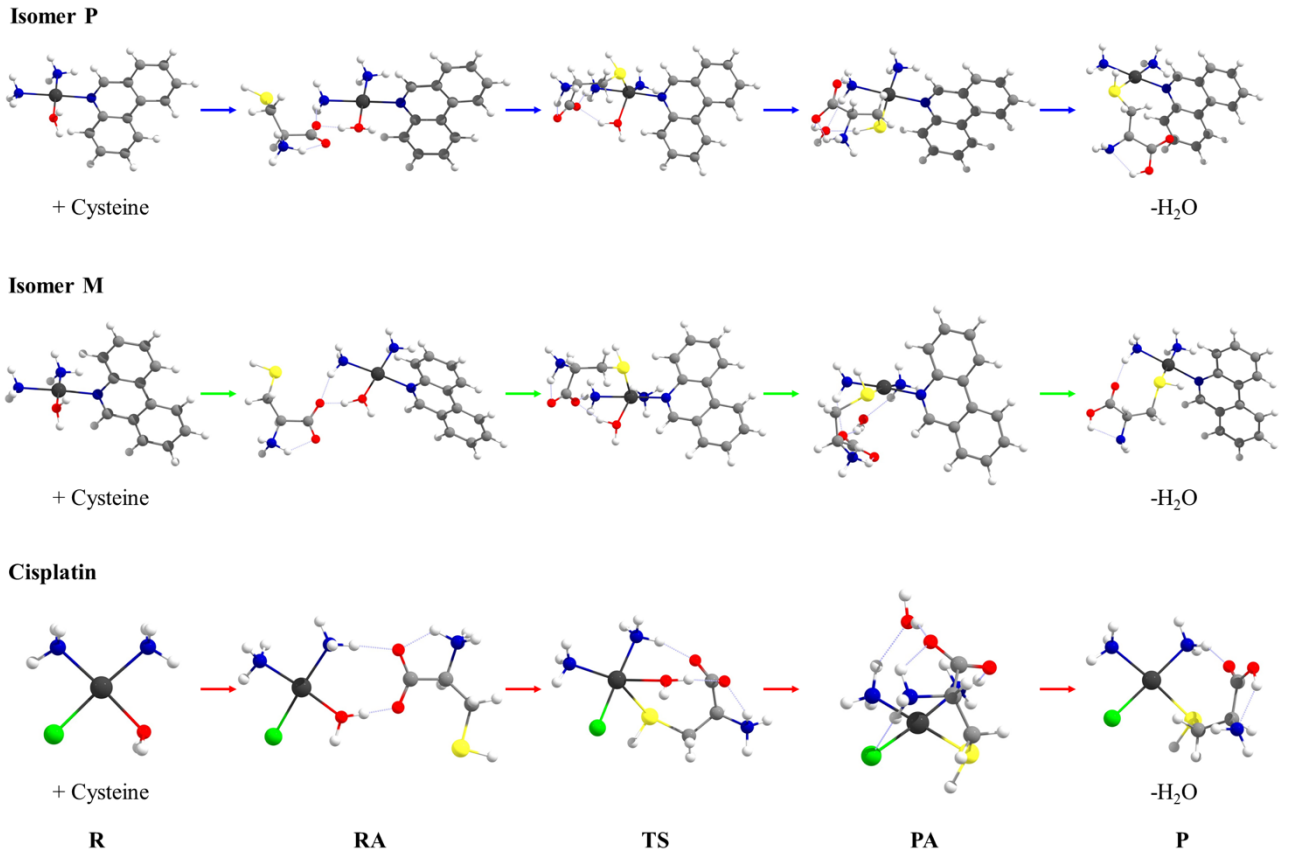


**Figure S6** Optimized structures for the reaction between isomer **phenPt**-P, isomer **phenPt**-M, **cisPt** and cysteine.

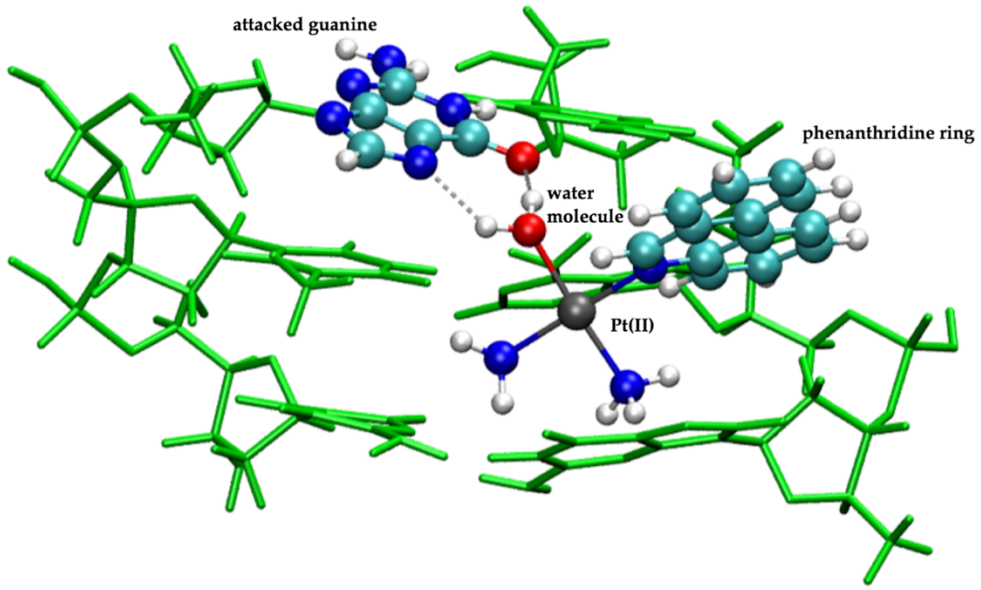


**Figure S7:** Minimum energy structures of the RA for the reaction between **phenPt** and a DNA fragment of three bases pair: color scheme: PM6 region in green, B3LYP region plotted in balls&sticks (green for carbon, blue for nitrogen, white for hydrogen, red for oxygen, and platinum in dark grey).

## 3. Optimized geometrical parameters

**Table S1** Comparison between calculated and experimental bond lengths (Å) and angles (°) for **phenPt**.

| Bond distance | Exp. | Calc. | Angles | Exp. | Calc. |
|---|---|---|---|---|---|
| Pt1-Cl | 2.296(7) | 2.318 | Cl1-Pt1-N1 | 90.25(6) | 85.170 |
| Pt1-N1 | 2.039(2) | 2.107 | Cl1-Pt1-N2 | 87.71(6) | 90.624 |
| Pt1-N2 | 2.025(2) | 2.064 | N1-Pt1-N3 | 89.08(8) | 95.280 |
| Pt1-N3 | 2.047(2) | 2.145 | N2-Pt1-N3 | 92.95(8) | 88.902 |

**Table S2** Relevant bond distances (Å) for isomer complex M with N7-Me-Gua , Nb is the entering nitrogen atom in N7 position of guanine, O(w) is the oxygen atom of water coordinated to Pt, with B3LYP and B3LYP-D3 functionals in water.

| **bond** | | **R** | **RA** | **RA (π-π)** | **TS** | **TS (π-π)** | **PA** | **P** |
|---|---|---|---|---|---|---|---|---|
| Pt-O(w) | B3LYP | 2.134 | 2.071 | 2.057 | 2.419 | - | 4.365 | - |
| | B3LYP-D3 | - | 2.067 | 2.060 | 2.372 | 2.373 | 4.125 | - |
| Pt-N1 | B3LYP | 2.127 | 2.120 | 2.112 | 2.085 | - | 2.091 | 2.101 |
| | B3LYP-D3 | - | 2.118 | 2.111 | 2084 | 2.0844 | 2.090 | - |
| Pt-N2 | B3LYP | 2.060 | 2.064 | 2.065 | 2.080 | - | 2.086 | 2.078 |
| | B3LYP-D3 | - | 2.062 | 2.067 | 2.074 | 2.0744 | 2.081 | - |
| Pt-N3 | B3LYP | 2.062 | 2.090 | 2.092 | 2.083 | - | 2.108 | 2.109 |
| | B3LYP-D3 | - | 2.092 | 2.094 | 2.084 | 2.085 | 2.110 | - |
| Pt- Nb | B3LYP | - | 4.262 | 4.429 | 2.637 | - | 2.063 | 2.065 |
| | B3LYP-D3 | - | 4.127 | 3.999 | 2.560 | 2.598 | 2.048 | - |

**Table S3** Relevant bond distances (Å) for isomer M with N7-Me-Ade , Nb is the entering nitrogen atom in N7 position of adenine, O(w) is the oxygen atom of water coordinated to Pt, with B3LYP and B3LYP-D3 functionals in water.

| **bond** | | **R** | **RA** | **RA (π-π)** | **TS** | **TS (π-π)** | **PA** | **P** |
|---|---|---|---|---|---|---|---|---|
| Pt-O(w) | B3LYP | 2.134 | 2.047 | 2.046 | 2.394 | - | 4.287 | - |
| | B3LYP-D3 | - | 2.042 | 2.040 | 2.350 | 2.354 | 4.072 | - |
| Pt-N1 | B3LYP | 2.127 | 2.114 | 2.114 | 2.101 | - | 2.107 | 2.117 |
| | B3LYP-D3 | - | 2.114 | 2.111 | 2.101 | 2.101 | 2.107 | - |
| Pt-N2 | B3LYP | 2.060 | 2.069 | 2.096 | 2.073 | - | 2.081 | 2.074 |
| | B3LYP-D3 | - | 2.067 | 2.067 | 2.067 | 2.068 | 2.075 | - |
| Pt-N3 | B3LYP | 2.062 | 2.114 | 2.115 | 2.087 | - | 2.114 | 2.114 |
| | B3LYP-D3 | - | 2.113 | 2.117 | 2.090 | 2.089 | 2.116 | - |
| Pt- Nb | B3LYP | - | 4.405 | 4.375 | 2.679 | - | 2.053 | 2.057 |
| | B3LYP-D3 | - | 4.269 | 3.987 | 2.632 | 2.635 | 2.040 | - |

**Table S4** Relevant bond distances (Å) for isomer M with N1-Me-Ade, Nb is the entering nitrogen atom in N1 position of adenine, O(w) is the oxygen atom of water coordinated to Pt with B3LYP and B3LYP-D3 functionals in water.

| bond | | R | RA | RA (π-π) | TS | TS (π-π) | PA | P |
|---|---|---|---|---|---|---|---|---|
| Pt-O(w) | B3LYP | 2.134 | 2.045 | 2.046 | 2.392 | - | 4.126 | - |
| | B3LYP-D3 | - | 2.035 | 2.036 | 2.364 | 2.447 | 4.048 | - |
| Pt-N1 | B3LYP | 2.127 | 2.108 | 2.104 | 2.103 | - | 2.111 | 2.123 |
| | B3LYP-D3 | - | 2.119 | 2.110 | 2.103 | 2.102 | 2.110 | - |
| Pt-N2 | B3LYP | 2.060 | 2.067 | 2.070 | 2.073 | - | 2.077 | 2.069 |
| | B3LYP-D3 | - | 2.062 | 2.067 | 2.067 | 2.069 | 2.072 | - |
| Pt-N3 | B3LYP | 2.062 | 2.117 | 2.117 | 2.089 | - | 2.122 | 2.125 |
| | B3LYP-D3 | - | 2.117 | 2.120 | 2.091 | 2.083 | 2.123 | - |
| Pt- Nb | B3LYP | - | 4.809 | 4.381 | 2.697 | - | 2.071 | 2.070 |
| | B3LYP-D3 | - | 4.352 | 3.964 | 2.637 | 2.675 | 2.066 | - |

**Table S5** Relevant bond distances (Å) for the first step of the reaction between N7-Me-Gua and **cisPt**, Nb is the entering nitrogen atom in N7 position of guanine, O(w) is the oxygen atom of water coordinated to Pt, with B3LYP and B3LYP-D3 functionals in water.

| bond | | R | RA | TS | PA | P |
|---|---|---|---|---|---|---|
| Pt-O(w) | B3LYP | 2.132 | 2.085 | 2.386 | 3.803 | - |
| | B3LYP-D3 | - | 2.082 | 2.358 | 4.284 | - |
| Pt-N1 | B3LYP | 2.137 | 2.113 | 2.123 | 2.106 | 2.115 |
| | B3LYP-D3 | - | 2.110 | 2.123 | 2.107 | - |
| Pt-N2 | B3LYP | 2.052 | 2.067 | 2.073 | 2.084 | 2.092 |
| | B3LYP-D3 | - | 2.071 | 2.077 | 2.101 | - |
| Pt-Cl | B3LYP | 2.309 | 2.329 | 2.328 | 2.352 | 2.339 |
| | B3LYP-D3 | - | 2.328 | 2.326 | 2.346 | - |
| Pt- Nb | B3LYP | - | 3.949 | 2.578 | 2.076 | 2.066 |
| | B3LYP-D3 | - | 3.734 | 2.560 | 2.052 | - |

**Table S6** Relevant bond distances (Å) for the second step of the reaction between N7-Me-Gua and **cisPt**, Nb is the entering nitrogen atom in N7 position of guanine, O(out) is the leaving oxygen atom of water, with B3LYP and B3LYP-D3 functionals in water.

| bond | | RA | TS | PA |
|---|---|---|---|---|
| Pt-O(out) | B3LYP | 2.029 | 2.385 | 4.165 |
| | B3LYP-D3 | 2.026 | 2.367 | 3.983 |
| Pt-N1 | B3LYP | 2.043 | 2.046 | 2.052 |
| | B3LYP-D3 | 2.041 | 2.044 | 2.050 |
| Pt-N2 | B3LYP | 2.111 | 2.105 | 2.100 |
| | B3LYP-D3 | 2.111 | 2.109 | 2.110 |
| Pt-O | B3LYP | 2.143 | 2.132 | 2.118 |
| | B3LYP-D3 | 2.145 | 2.132 | 2.130 |
| Pt- Nb | B3LYP | 4.333 | 2.521 | 2.065 |
| | B3LYP-D3 | 4.253 | 2.494 | 2.055 |

## 4. Imaginary frequencies (TS)

**Table S7**: Computed imaginary frequencies ($cm^{-1}$) for the TS along with the reactions of **phenPt** and **cisPt** in water.

| | B3LYP | B3LYP-D3 |
|---|---|---|
| Isomer-P + $H_2O$ | 161.6 | - |
| Isomer-M + $H_2O$ | 167.0 | - |
| **cisPt** + $H_2O$ | 181.5 | - |
| Isomer-P + N7-Me-Gua | 150.0 | - |
| Isomer-M + N7-Me-Gua | 145.6 | 140.2 |
| Isomer-M + N7-Me-Gua (π-π) | - | 140.4 |
| $[Pt(NH_3)_2(H_2O)Cl]^+$ + N7-Me-Gua | 149.0 | 145.2 |
| $[Pt(NH_3)_2(H_2O)_2]^{2+}$ + N7-Me-Gua | 157.7 | 153.3 |
| Isomer-P + N7-Me-Ade | 145.3 | - |
| Isomer-M + N7-Me-Ade | 147.6 | 143.1 |
| Isomer-M + N7-Me-Ade (π-π) | - | 148.7 |
| Isomer-P + N1-Me-Ade | 141.6 | - |
| Isomer-M + N1-Me-Ade | 136.3 | 135.8 |
| Isomer-M + N1-Me-Ade (π-π) | - | 180.8 |
| Isomer-P + cyst | 146.7 | - |
| Isomer-M + cyst | 141.0 | - |
| **cisPt** + cyst | 148.2 | - |

**5. Relative Gibbs free energies (reaction profile)**

The kinetic and thermodynamic values reported in the main text are based on the computed RA→TS and TS→PA barriers at B3LYP and B3LYP-D3 levels of theory. Although B3LYP functional may produce meaningful geometries and relative energies in the reaction of platinum-based complexes, it is known to fail when assessing π-π contacts.[17] The performed calculations are fully consistent with that previous findings. Indeed, the optimization of starting structures with geometry suitable for the interaction with π-π between **phenPt** and Me-Gua and Me-Ade (Fig. S5-D, -E and -F) quickly back to structures of RAs without stacking (Fig. S5-A, -B and -C, respectively) if B3LYP is used. On the contrary, B3LYP-D3 optimizations not only retain the stacked forms but also predict an additional stabilization due to the π-π contact established between the DNA base and the phenanthridine ring, which in turn increase the energetic barrier and slow down the reaction (see main text and Table S9).

Aiming to extract a more general conclusion about the ability of the DFT methods to mimic the reactivity of monofunctional platinum anticancer drugs, Table S10 summarizes the computed activation delivered by B3LYP-D3 and compares these values with the obtained with the ωB97X-D functional. A similar trend is observed –if calculations are performed with non-stacked system [Isomer-M+N7-Me-Gua], the computed activation energies with B3LYP-D3 and ωB97X-D differ in less than one kcal $mol^{-1}$ unit, 15.2 and 14.5 kcal $mol^{-1}$, respectively. As a consequence, the associated rate constants largely overestimate the experimental value by 6-7 order of magnitude. However, the use of either B3LYP-D3 or ωB97X-D approach with the stacked-RA model [Isomer-M+N7-Me-Gua (π-π)] significantly increase the energetic barrier (20.3 and 22.5 kcal $mol^{-1}$, respectively), which in turn recovers the reconciliation between theoretical and experimental kinetic parameters. All these findings allow us to conclude that the π-π interaction between DNA bases and the phenanthridine ring plays a pivotal role in the reaction. Accurate theoretical schemes, e.g., range-separated functionals and/or Grimme's empirical dispersion corrections, are therefore essential to reach valuable predictions in **phenPt**-like model systems.

Table S10 also includes the predictions for the reactions of **cisPt** with a guanine base. As one can see, the numeric outputs obtained with either B3LYP-D3 or ωB97X-D perfectly match the available experimental data, which confirm the validity of these methods in the simulation of platinum-based drugs.

**Table S8** Relative Gibbs free energy values (kcal mol$^{-1}$), associated to the hydrolysis reaction pathway for P and M isomer of **phenPt** and **cisPt**, in PCM water, at B3LYP.

| G | | R → RA | RA → TS | TS → PA | PA → P |
|---|---|---|---|---|---|
| Isomer P | B3LYP | 6.9 | 25.2 | -14.6 | 1.3 |
| | B3LYP-D3 | - | 23.2 | -11 | - |
| Isomer M | B3LYP | 6.6 | 26.3 | -15.2 | 0.9 |
| | B3LYP-D3 | - | 24.3 | -13.2 | - |
| Cisplatin | B3LYP | 6.7 | 24.5 | -18.5 | 2.6 |
| | B3LYP-D3 | - | 24.0 | -18.5 | - |

**Table S9:** Relative Gibbs free energy values (kcal mol$^{-1}$), associated to the reaction between N7-Me-Gua, N7-Me-Ade, N1-Me-Ade and isomer P and isomer M of **phenPt** and **cisPt**, at B3LYP and B3LYP-D3 in PCM water. [a]

| | **B3LYP** | | | |
|---|---|---|---|---|
| | **R → RA** | **RA → TS** | **TS → PA** | **PA →P** |
| Isomer-P + N7-Me-Gua | -2.0 | 21.2 | -31.5 | -5.5 |
| Isomer-M+ N7-Me-Gua | -0.7 | 19.5 | -31.4 | -5.3 |
| Isomer-P + N7-Me-Ade | 4.5 | 23.7 | -33.6 | -5.0 |
| Isomer-M + N7-Me-Ade | 4.3 | 22.8 | -33.8 | -4.8 |
| Isomer-P + N1-Me-Ade | 0.0 | 27.4 | -34.9 | -4.3 |
| Isomer-M + N1-Me-Ade | 1.2 | 26.5 | -34.7 | -6.4 |
| Cisplatin + N7-Me-Gua | -2.5 | 21.5 | -29.6 | -7.3 |

| | **B3LYP-D3** | | | |
|---|---|---|---|---|
| | **R → RA** | **RA → TS** | **TS → PA** | **PA →P** |
| Isomer-M+ N7-Me-Gua | - | 15.2 | -30.5 | - |
| Isomer-M + N7-Me-Ade | - | 17.1 | -33.0 | |
| Isomer-M + N1-Me-Ade | - | 19.1 | -32.7 | - |
| Isomer-M+ N7-Me-Gua (π-π) | - | 20.3 | -30.4 | |
| Isomer-M + N7-Me-Ade (π-π) | - | 23.0 | -32.3 | - |
| Isomer-M + N1-Me-Ade(π-π) | - | 25.8 | -32.4 | - |
| Cisplatin + N7-Me-Gua | - | 17.8 | -28.0 | - |

(a) The π–π stacked reactive adducts are not stable at the B3LYP level of theory (see text).

**Table S10:** Computed relative Gibbs free energy values (ΔG, kcal $mol^{-1}$) and rate constants (k, $s^{-1}$) for to the reaction between isomer M of **phenPt** and **cisPt**, with B3LYP-D3 and ωB97X-D in PCM water.

| | ΔG | | k | | |
|---|---|---|---|---|---|
| | B3LYP-D3 | ω-B97XD | B3LYP-D3 | ω-B97XD | exp[a] |
| Isomer-M+ N7-Me-Gua | 15.2 | 14.5 | $4.49 \times 10^{1}$ | $1.46 \times 10^{2}$ | $3.6 \times 10^{-5}$ |
| Isomer-M+ N7-Me-Gua (π-π) | 20.3 | 22.5 | $8.21 \times 10^{-3}$ | $2.01 \times 10^{-4}$ | |
| Cisplatin + N7-Me-Gua | 17.8 | 17.9 | $5.58 \times 10^{-1}$ | $4.71 \times 10^{-1}$ | $1.2 – 2.8 \times 10^{-1}$ |

(a) Experimental values are taken from references 26 and 27.

**Table S11:** Relative Gibbs free energy values (kcal $mol^{-1}$), associated to the reaction between cysteine and isomer P and isomer M of **phenPt** and **cisPt**, at B3LYP and B3LYP-D3 in PCM water.

| | | **R → RA** | **RA → TS** | **TS → PA** | **PA → P** |
|---|---|---|---|---|---|
| isomer P | B3LYP | 0.5 | 24.9 | -22.1 | -7.3 |
| | B3LYP-D3 | - | 19.4 | -24.9 | - |
| isomer M | B3LYP | 0.8 | 24.3 | -22.6 | -9.5 |
| | B3LYP-D3 | - | 18.9 | -27.3 | - |
| cisplatin | B3LYP | 0.1 | 25.4 | -27.7 | -6.8 |
| | B3LYP-D3 | - | 20.9 | -33.0 | - |

## Bibliography


(1) Jamieson, E. R.; Lippard, S. J. Structure, Recognition, and Processing of Cisplatin-DNA Adducts. *Chem. Rev.* **1999**, *99* (9), 2467–2498.

(2) Becke, A. D. Density-functional Thermochemistry. III. The Role of Exact Exchange. *J. Chem. Phys.* **1993**, *98* (7), 5648–5652.

(3) Lee, C.; Yang, W.; Parr, R. G. Development of the Colle-Salvetti Correlation-Energy Formula into a Functional of the Electron Density. *Phys. Rev. B* **1988**, *37* (2), 785–789.

(4) Gaussian 16, Revision A.03, Frisch, M. J.; Trucks, G. W.; Schlegel, H. B.; Scuseria, G. E.; Robb, M. A.; Cheeseman, J. R.; Scalmani, G.; Barone, V.; Petersson, G. A.; Nakatsuji, H.; Li, X.; Caricato, M.; Marenich, A. V.; Bloino, J.; Janesko, B. G.; Gomperts, R.; Mennucci, B.; Hratchian, H. P.; Ortiz, J. V.; Izmaylov, A. F.; Sonnenberg, J. L.; Williams-Young, D.; Ding, F.; Lipparini, F.; Egidi, F.; Goings, J.; Peng, B.; Petrone, A.; Henderson, T.; Ranasinghe, D.; Zakrzewski, V. G.; Gao, J.; Rega, N.; Zheng, G.; Liang, W.; Hada, M.; Ehara, M.; Toyota, K.; Fukuda, R.; Hasegawa, J.; Ishida, M.; Nakajima, T.; Honda, Y.; Kitao, O.; Nakai, H.; Vreven, T.; Throssell, K.; Montgomery, J. A., Jr.; Peralta, J. E.; Ogliaro, F.; Bearpark, M. J.; Heyd, J. J.; Brothers, E. N.; Kudin, K. N.; Staroverov, V. N.; Keith, T. A.; Kobayashi, R.; Normand, J.; Raghavachari, K.; Rendell, A. P.; Burant, J. C.; Iyengar, S. S.; Tomasi, J.; Cossi, M.; Millam, J. M.; Klene, M.; Adamo, C.; Cammi, R.; Ochterski, J. W.; Martin, R. L.; Morokuma, K.; Farkas, O.; Foresman, J. B.; Fox, D. J. Gaussian, Inc., Wallingford CT, 2016.

(5) Baik, M. H.; Friesner, R. a.; Lippard, S. J. Theoretical Study of Cisplatin Binding to Purine Bases: Why Does Cisplatin Prefer Guanine over Adenine? *J. Am. Chem. Soc.* **2003**, *125* (46), 14082–14092.

(6) Raber, J.; Zhu, C. B.; Eriksson, L. A. Theoretical Study of Cisplatin Binding to DNA: The Importance of Initial Complex Stabilization. *J. Phys. Chem. B* **2005**, *109* (21), 11006–11015.

(7) Costa, L. A.; Hambley, T. W.; Rocha, W. R.; De Almeida, W. B.; Dos Santos, H. F. Kinetics and Structural Aspects of the Cisplatin Interactions With Guanine : A Quantum Mechanical Description. *Int. J. Quantum Chem.* **2006**, *106* (9), 2129–2144.

(8) Alberto, M. E.; Lucas, M. F. A.; Pavelka, M.; Russo, N. The Second-Generation Anticancer Drug Nedaplatin: A Theoretical Investigation on the Hydrolysis Mechanism. *J. Phys. Chem. B* **2009**, *113* (43), 14473–14479.

(9) Alberto, M. E.; Butera, V.; Russo, N. Which One among the Pt-Containing Anticancer Drugs More Easily Forms Monoadducts with G and A DNA Bases? A Comparative Study among Oxaliplatin, Nedaplatin, and Carboplatin. *Inorg. Chem.* **2011**, *50* (15), 6965–6971.

(10) Alberto, M. E.; Cosentino, C.; Russo, N. Hydrolysis Mechanism of Anticancer Pd ( II ) Complexes with Coumarin Derivatives : A Theoretical Investigation. *Struct Chem* **2012**, *23*, 831–839.

(11) Chen, B.; Zhou, L. Computational Study on Mechanisms of the Anticancer Drug: Cisplatin and Novel Polynuclear platinum(II) Interaction with Sulfur-Donor Biomolecules and {DNA} Purine Bases. *Comput. Theor. Chem.* **2015**, *1074*, 36–49.

(12) Graziani, V.; Coletti, C.; Marrone, A.; Re, N. Activation and Reactivity of a Bispidine Analogue of Cisplatin : A Theoretical Investigation. *J. Phys. Chem. A* **2016**, *120* (27), 5175–5186.

(13) Reddy, V. P.; Mitra, I.; Mukherjee, S.; Sengupta, P. S.; Dodda, R.; Moi, S. C. A Theoretical Investigation on Hydrolysis Mechanism of Biologically Relevant Pt ( II ) / Pd ( II ) Complexes with σ - Donor and π -Acceptor Carrier Ligand. *Chem. Phys. Lett.* **2016**, *657* (16), 148–155.

(14) Mitra, I.; Reddy, V. P. B.; Mukherjee, S.; Linert, W.; Moi, S. C. Hydrolysis Theory Based on Density Functional Studies for Cytotoxic Pt ( II ) and Pd ( II ) Complexes with Benzimidazole Derivative. *Chem. Phys. Lett.* **2017**, *678* (16), 250–258.

(15) Mukherjee, S.; B, V. P. R.; Mitra, I.; Linert, W.; Moi, S. C. Hydrolysis Mechanism of ( N , N ) Chelated Cytotoxic Pt / Pd ( II ) - Dichloro Complexes : A Theoretical Approach. *Chem. Phys. Lett.* **2017**, *678*, 241–249.

(16) Burda, J. V.; Zeizinger, M.; Leszczynski, J. Hydration Process as an Activation of Trans- And Cisplatin Complexes in Anticancer Treatment. DFT and Ab Initio Computational Study of Thermodynamic and Kinetic Parameters. *J. Comput. Chem.* **2005**, *26*, 907–914.

(17) Grimme, S.; Ehrlich, S.; Goerigk, L. Effect of the Damping Function in Dispersion Corrected Density Functional Theory. *J. Comput. Chem.* **2011**, *32* (1), 1456–1465.

(18) Chai, J.D.; Head-Gordon, M. Long-range corrected hybrid density functionals with damped atom-atom dispersion corrections. *Phys. Chem. Chem. Phys.* **2008**, 10, 6615–6620.

(19) Andrae, D.; Häußermann, U.; Dolg, M.; Stoll, H.; Preuß, H. Energy-Adjusted Ab Initio Pseudopotentials for the Second and Third Row Transition Elements. *Theor. Chim. Acta* **1990**, *77* (2), 123–141.

(20) Melchior, A.; Martínez, J. M.; Pappalardo, R. R.; Sánchez Marcos, E. Hydration of Cisplatin Studied by an Effective Ab Initio Pair Potential Including Solute-Solvent Polarization. *J. Chem. Theory Comput.* **2013**, *9* (10), 4562–4573.

(21) Melchior, A.; Peralta, E.; Valiente, M.; Tavagnacco, C.; Endrizzi, F.; Tolazzi, M. Interaction of d10 Metal Ions with Thioether Ligands: A Thermodynamic and Theoretical Study. *Dalt. Trans.* **2013**, *42*, 6074–6082.

(22) Melchior, A.; Sánchez Marcos, E.; R. Pappalardo, R.; Martínez, J. M. Comparative Study of the Hydrolysis of a Third- and a First-Generation Platinum Anticancer Complexes. *Theor. Chem. Acc.* **2011**, *128* (4–6), 627–638.

(23) Tomasi, J.; Mennucci, B.; Cammi, R. Quantum Mechanical Continuum Solvation Models. *Chem. Rev.* **2005**, *105* (8), 2999–3093.

(24) Dapprich, S.; Komáromi, I.; Byun, K. S.; Morokuma, K.; Frisch, M. J. A New ONIOM Implementation in Gaussian98. Part I. The Calculation of Energies, Gradients, Vibrational Frequencies and Electric Field Derivatives. *J. Mol. Struct. THEOCHEM* **1999**, *461–462*, 1–21.

(25) Stewart, J. J. P. Optimization of Parameters for Semiempirical Methods V: Modification of NDDO Approximations and Application to 70 Elements. *J. Mol. Model.* **2007**, *13* (12), 1173–1213.

(26) Legendre, F.; Bas, V.; Kozelka, J.; Chottard, J. C. A complete kinetic study of GG versus AG plantination suggests that the doubly aquated derivatives of cisplatin are the actual DNA binding species. *Chem. Eur. J.* **2000**, 6, 2002–2010.